Optical Fiber Systems for the BigBOSS Instrument

Jerry Edelstein[1], Claire Poppett[2], Martin Sirk[1], Robert Besuner[1], Robin Lafever[2], Jeremy R. Allington-Smith[3], Graham J. Murray[3]

[1]University of California Berkeley, Space Sciences Laboratory
[2]Lawrence Berkeley National Laboratory
[3]Durham University

ABSTRACT

We describe the fiber optics systems for use in BigBOSS, a proposed massively parallel multi-object spectrograph for the Kitt Peak Mayall 4-m telescope that will measure baryon acoustic oscillations to explore dark energy. BigBOSS will include 5,000 optical fibers each precisely actuator-positioned to collect an astronomical target's flux at the telescope prime-focus. The fibers are to be routed 40m through the telescope facility to feed ten visible-band imaging spectrographs. We report on our fiber component development and performance measurement program. Results include the numerical modeling of focal ratio degradation (FRD), observations of actual fibers' collimated and converging beam FRD, and observations of FRD from different types of fiber terminations, mechanical connectors, and fusion-splice connections.

Keywords: Optical fiber, BigBOSS, multi-object spectrograph, focal ratio degradation, fusion splicing

1 INTRODUCTION

BigBOSS is a proposed instrument[1] for the Kitt Peak National Observatory's 4-m Mayall telescope to explore dark energy using the baryon acoustic oscillation method, measuring the red-shift of tens of millions of galaxies over five years. In BigBOSS, a 5,000 unit fiber optic system transmits target flux from the focal plane to remotely located visible passband spectrographs. This paper describes the requirements for the fiber optics system, discusses the present system and element design solutions, and details results from our related development and performance measurement programs.

For BigBOSS at the Mayall telescope, the primary mirror and a new prime-focus optical corrector[2] will provide an image of the sky over a 3° field of view to a convex focal surface. Target radiation reaches the focal plane with an f/4.5 cone having a chief-ray normal to the surface within of 0.5 degrees. This light is to be injected to the BigBOSS fibers. To collect this light, each science fiber is independently positioned within a fixed patrol radius by an actuator affixed to the focal plane. Instrument simulations and science optimization analyses show that the fiber should collect science target radiation within a 120 um diameter at the focal plane. Groups of 500 fibers are gathered from the opposite side of the focal plane into junction boxes where they are connected and bundled into ten rugged cables. These cables traverse the primary cage spider and the telescope into an optics laboratory where, after a 40-m run, they are terminated into a linear spectrograph slit array. Each slit arrays feeds a slit-imaging multi-band f/4 spectrograph[3] so that 5,000 medium resolution spectra covering a 360 to 980 nm passband can be simultaneously obtained. An overall illustration of the fiber system installation within BigBOSS and a fiber system schematic are shown in Figure 1.

The general requirements for the fiber system are:

- Quantity 5,000 science fibers
- Operating wavelengths 360 - 980 nm
- Fiber optical input f/4.5 @ < 0.5 deg telecentricity
- Fiber core diameter of 120 μm
- Fiber run length 40-m
- *S*ets of 500 fibers outputs arranged to the spectrograph slit surface
- Fiber optical output to a common f/4.0 pupil

Fiber connection to facilitate actuator installation and test.
Fiber system throughput 90%, excluding bulk transmission loss.

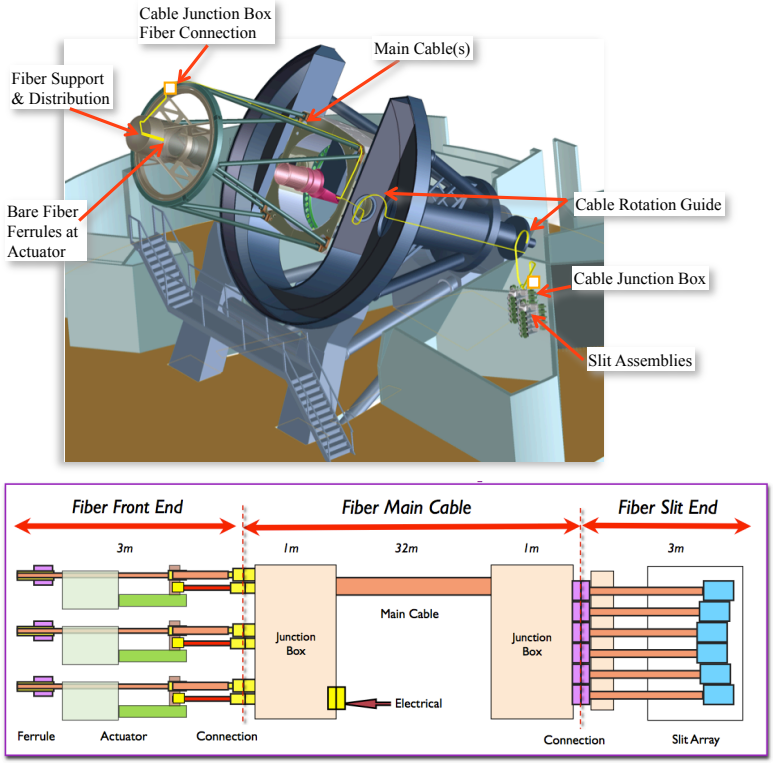

Figure 1: The main elements of the the BigBOSS fiber system are illustrated in place on the Mayall Telescope (top panel). A schematic diagram of the fiber system (bottom panel) shows the fiber front end that interfaces to the focal plane, the fiber main cable that traverses the facility, and the fiber slit end which interfaces to the spectrographs.

2 OPTICAL FIBER AND THROUGHPUT

Fiber throughput is science critical as light loss requires longer exposure times with a lower survey rates, limiting to the rate of sky coverage. Fiber throughput is effected by the fiber glass bulk transmission and losses at the fiber terminations due to polishing imperfections, and Fresnel losses. Angular scattering induced by the fiber (i.e. focal ratio degradation, or "FRD") can also degrade throughput if light is deviated beyond the acceptance angle of the subsequent optical system. The FRD is caused in part by imperfections in the fiber manufacturing process and often most significantly by the fiber-end treatment, e.g., bonding and polishing stresses induced on a fiber's terminus. FRD can also be exacerbated by stresses, bends and micro-cracks caused by fiber handling and routing. The apparent FRD is also impacted by off-axis injection of the light-cone coming from the telescope, i.e. its non-telecentricity to the fiber axis. The most extreme angles of injection to a fiber sets the most extreme angle from the fiber output. We used simulation results, shown in Figure 2, and values from our experience with BOSS to establish FRD performance parameters that 90% of f/4.5 input flux will be projected within the f/4.0 acceptance of the spectrograph, including angular allowances for fiber injection and output. This moderate-resolution spectrograph is expected to be insensitive to variations in pupil uniformity.

2.1 The Optical Fiber

The optical fiber material selection is driven by the following demands:

Maximized bulk transmission
Minimized spectral absorption features
Low intrinsic focal ratio degradation

Fiber outside diameter < 240 μm for spectrograph slit spacing

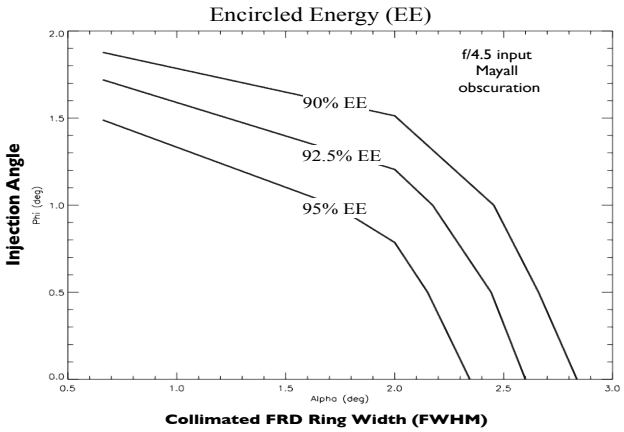

Figure 2: Fiber system throughput depends on both FRD and injection angle error. The contours show results from numerical modeling which shows the energy encircled within an f/4.0 aperture given an f/4.5 input illumination that includes a central obscuration corresponding to that for the Mayall telescope. Energy is lost at the aperture due to beam spreading caused by inherent FRD and the telecentric angle of fiber injection. The FRD is characterized by the width of the circular ring produced by azimuthally scrambled collimated input to the fiber. Fibers with high quality finish have collimated FRD ring width of < 1°. For example, the figures shows that if given a collimated FRD of 1.5° then > 95% encircled energy can be recovered if the injection angle error is < 1.1°.

Survival of repeated actuator flexing (~30k cycles)

We have selected low-OH silica fiber that transmits the desired pass band while lacking the significant absorption features inherent in high-OH, UV enhanced fibers. The selected baseline fiber is Polymicro FBP with diameters of 120 μm core, 170 μm clad, and a 190 μm polyimide jacket. The fiber bulk transmission is show in Figure 3. This particular fiber has been shown to have low intrinsic focal ratio degradation during extensive use in the BOSS project. The fiber is drawn with a proprietary process that is designed to minimize focal ratio degradation by alleviating stress in the fiber. We also investigated the possibility of using hydrogen soaked, low-OH fibers that promised a UV transmission enhancement[4]. Unfortunately, we were unable to find a current manufacturer of this

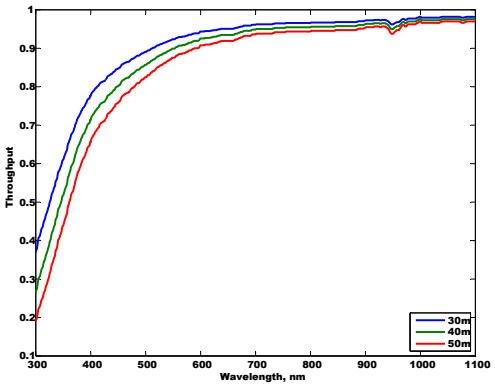

Figure 3: Bulk transmission of of Polymicro FBP fiber. Predicted transmission for the 40-m BigBOSS fiber is 55% at the 360nm working pass band edge.

type of fiber or to allay concerns that, given a small diameter fiber, the enhancement would dissipate on this projects multi-year timescale due to hydrogen diffusion from the fiber core.

3 FRONT-END FIBER ASSEMBLY

At the focal plane, each fiber end is terminated with a ferrule and attached to a 2-axis positioner with mechanical requirements:

Ferrule mount to actuator removable from and insertable through the actuator (< 1.25mm diameter)
Permit actuator installation from the focal plane optical face
Operational temperature range -10° to +20°C

The front-end fiber assembly also has optical requirements:

Fiber output face, flat polished, AR coated (360–980 nm) < 1.5% total loss per coating
FRD 92.5% EE within f/4.0 for f/4.5 input, including connections
Ferrule 5 μm axial position accuracy in actuator to match focal plane
Fiber optical axis alignment to actuator ± 0.5°

The front end fiber unit is illustrated in Figure 4. The fiber is to be bonded into a ferrule, followed by polishing to a flat optical surface. To maximize throughput, an antireflection (AR) coating will be applied to the polished fiber ends. The process and materials used in bonding and polishing steps can induce surface stress and damage, potentially negatively impacting FRD and optical scattering performance. High quality fiber assemblies have been achieved using combinations of specific fiber glasses, fiber buffers and ferrule materials in combination with specialized epoxies and curing conditions. Critical factors include the balance of material's coefficient of thermal expansion (CTE) and adhesive shrinkage, strength and modulus. We intend to use a ceramic ferrule together with a polyimide buffered fiber. Ceramic has a similar expansion coefficient to glass. Compared to acrylic or epoxy buffers, polyimide has high diametrical and concentric tolerances and high stiffness, which allows for both bonding the un-stripped, buffered fiber within the ferrule and for good optical quality end-polishing, respectively. Furthermore, polyimide can survive higher temperatures in the AR coating process applied after polishing.

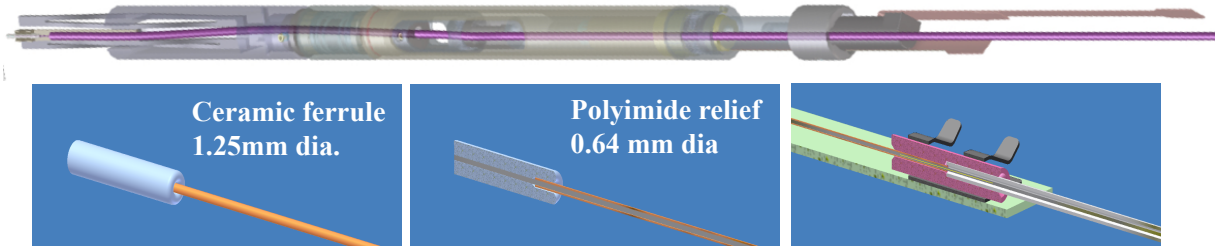

Figure 4: The front end fiber assembly feeds through a position actuator (above) and terminates at a polished end ceramic ferrule (left). The fiber is strain relieved with a loose outer sleeve of polyimide (center) that transitions to furcation tubing at an adapter fixed to the aft of the actuator (right).

The ferrule will be coupled to the metal actuator arm using an actuator assembly jig to provide a 5 μm axial location precision for matching the focal plane surface and 0.5° optical axis alignment for input telecentricity requirements. The lateral fiber-end positioning accuracy is less critical because a fiber tracking camera will calibrate the fiber's lateral position. Nonetheless, the position needs to be repeatable and stable between camera calibrations. A low-stress semi-kinematic actuator interface fitment will be used so that stress or motion will not be induced at the fiber tip over the thermal range found at prime focus. A protective strain sleeve is bonded to the ferrule in order to relieve the potential of a high-stress, FRD inducing region where the fiber enters the ferrule assembly. The strain relief sleeve must be small enough to pass through the actuator, flexible enough to allow for unimpeded movement within the actuator, and have adequate wear resistance. We intend to use an oversized polyimide tube that transitions to a small plastic furcation tube at the actuator rear to protect the fibers during their collection and transit to junction boxes that commence the fiber cable run, as described below.

We consider the potential for a time dependent degradation of transmission efficiency over the course of the >20,000 cycles of motion as the fiber is flexed during actuator motion over the observation lifetime. The Polymicro FBP

fibers used for BOSS, a hard clad silica with a single hard polyimide overcoat, have proven robust to hand insertion flexing cycles. We are conducting degradation tests to determine fiber performance given the mechanical requirements of actuator motion cycles. For example, our preliminary results show no significant FRD degradation following 90,000 bending cycles of the FBP fiber at the minimum 5 cm radius bend to be induced by the actuator. The fibers will also be flexed in their bundled run assemblies as the telescope slews over the sky. These repeated motions will be constrained by guides belts, rails and soft clamps to radii that are relatively large compared to bends at the actuator. A fiber bundle assembly mock-up will be exercised over the designed routing system to verify its life performance.

4 FIBER CONNECTIONS AND TESTING

The ability to optically connect fibers will enable actuator installation from the focal plane's front optical face with the collection of fibers from the focal plane's rear face. Use of an optical fiber connection also disentangles the development paths for the focal plane, actuators, and spectrograph slit. However, fiber connections are expected to cause some bulk transmission losses and FRD degradation. We have been conducting an extensive experimental study of alternate connection implementations to see if they can meet our FRD requirements while limiting connection loss to < 2.5% (0.1 dB). Our tests include commercial single and multiple fiber mechanical connectors as well as the direct fusion splicing of fibers.

We have developed a fiber evaluation facility, schematically illustrated in Figure 5, that is used to evaluate FRD by two methods: 1) the collimated FRD method which finds the ring-width resulting from collimated off-axis fiber illumination at various fixed angles, and 2) the converging FRD method which finds the encircled energy ejected within a fixed focal ratio following conical illumination of the fiber at various f/#'s, including a central obscuration to simulate the telescope as desired. Although the converging FRD method more accurately represents the conditions in the final instrument, the collimated beam method is far more convenient because precise pre-alignment between the optical fiber axis and the converging illumination cone axis is not needed. This axial alignment is important because injection angle error will compound with the inherent FRD. We checked that the relationship between collimated and converging FRD is sound and that collimated FRD measured at the maximum input angle corresponding to f/4.5 would consistently predict converging FRD results. Our facility is also capable of imaging the

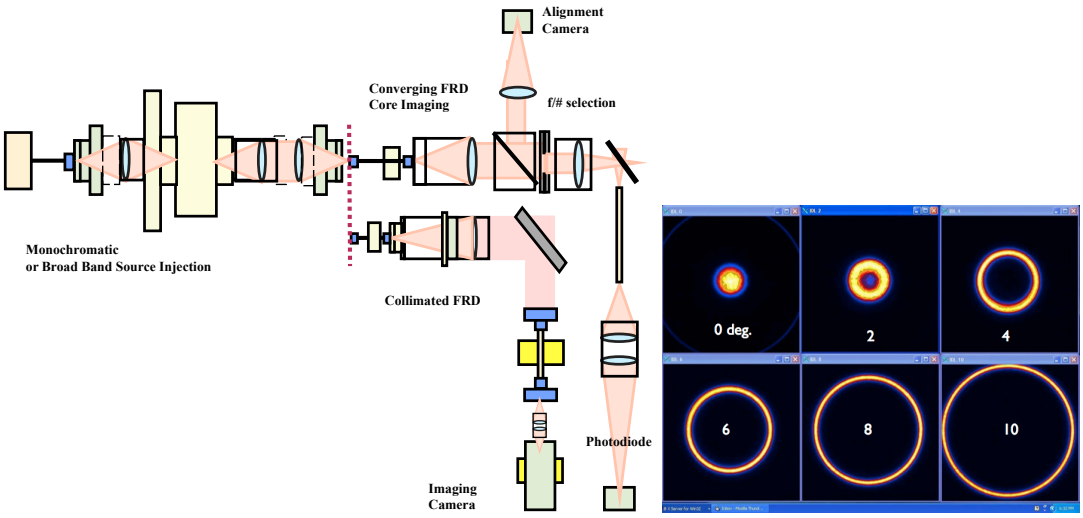

Figure 5. A schematic of the Fiber evaluation facility schematic (left panel) show that a light source (left) feeds a source fiber of chosen diameter which, in turn, illuminates either a collimated or converging optic (top right). The optics illuminate the fiber at a chosen input angle or f/#. An alignment camera is used to view the fiber tip illumination conditions. The fiber output is viewed (right) either in the far or near field with a camera or with a photodiode for throughput calibrations. Example data (right panel) of collimated FRD observations are shown at a variety of input angles (in degrees).

fiber output face at high resolution for near-field uniformity tests and of measuring bulk throughput by injecting flux completely within the fiber core and comparing its output to the source with a photodiode.
Bulk throughput losses from mechanical connectors can arise from the relative mis-centering of the mated fiber cores (geometric loss) and from Fresnel or spectral ringing if a gap exists between the fiber faces. A core offset of 1 µm corresponds to a bulk loss of ~1% for a 120 µm fiber core. Commercial mechanical connectors promise mechanical offsets of one to a few µm. Further offsets can occur due to fiber core centration and size tolerances. Air gaps and Fresnel losses may be mitigated by the using index coupling oils or gels, although they are prone to contamination by particulates. Mechanical connectors can also cause FRD degradation from termination end stress or from fiber optical axis misalignments.

We tested the FRD of fibers terminated with mechanical connectors using 120 µm core FBP fiber. The termination types include: 1) A high-quality 'standard' fiber terminated at each end with a stainless steel SMA or FC ferrule and

Connector type	**Uncoupled FRD** degree FWHM	**Coupled FRD** degree FWHM
FC + FC 'Standard'	0.6 - 0.7	-
MTP x 32 + SMA 'Standard'	0.5 - 1.8	2.0 - 3.9
DMI + DMI	2.5 - 3.5	3.4 - 4.3
GHD + GHD	-	> 5.5

Table I. Collimated FRD measurements of fibers terminated with mechanical connectors. Coupled mechanical connectors significantly degrade the FRD performance.

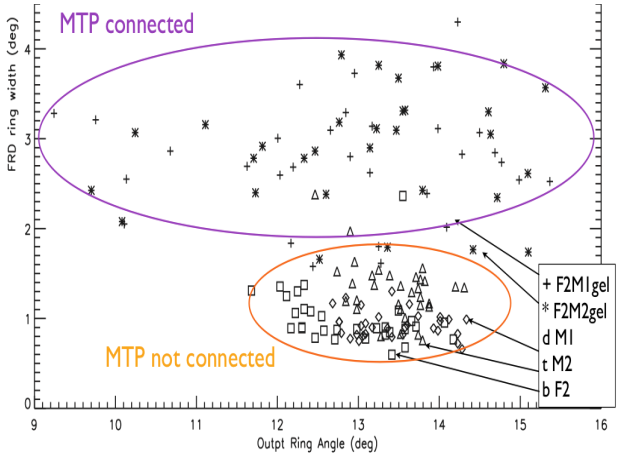

Figure 6. FRD testing results from MTP multiple-fiber connectors. The vertical axis shows the collimated FRD ring width (FWHM) in degrees. The horizontal axis shows the ring diameter. Results for uncoupled fibers are shown in the orange oval. Results for coupled connectors are shown in the purple oval with optical index matching gel filled connections denoted by a star. The coupled connection clearly degrades the FRD performance.

low-stress

epoxy bonding procedure that was developed for the BOSS program. 2) US Conec MTP connectors that simultaneously face-couple 32 fibers using an epoxy-bonded into monolithic precision-molded ferrules. The MTP connectors were fabricated using the same process as applied the APOGEE project. 3) Glenair GHD connectors, a single fiber connector that face-couples fibers which have been epoxy bonded and face polished to ceramic ferrules and are co-aligned with a ceramic sleeve. 4) Diamond S.A. DMI connectors, a single fiber connector that face-couples ceramic ferrules within a ceramic alignment sleeve. The DMI ferrules include a metal insert that is precision crimped by the manufacturer to accurately center the fiber and so that a μm-scale epoxy bond line remains between the fiber and the insert. We typically first measured the FRD of a single, 50 to 100 cm long uncoupled fiber that has been terminated at one or both ends with the test connector. This uncoupled performance represents a best FRD performance limit that can be compared directly to that of the quality standard termination. We then measure the FRD of a coupled fiber. Table I and Figure 6 shows results from mechanical connector fiber testing. The conclusion is that while uncoupled mechanically-terminated fibers have FRD comparable to the high-quality standard fiber, the coupled mechanical connectors we tested did not deliver the FRD performance needed to meet our requirements.

Fusion splicing is an alternate to mechanical connection. Fibers are stripped and cleaved, melted together, and then recoated for environmental protection. Fusion spliced fibers can suffer throughput losses from inclusions or imperfections at the fusion interface and from relative mis-centering of the fiber cores. Commercial splicers promise <1% loss for multimode fibers as geometric loss is minimized by μm-level pre-fuse core alignment and by surface tension induced fiber core centering during the fusion glass melt. The impact of fusion splicing on FRD has not been clearly reported in the literature. Fusion splicing may impact FRD by causing stress near the junction, by physically deforming the core-clade region, and by altering the fiber material indices of refraction due to heat induced migration of the clad or core dopants. Furthermore, each one of a variety of methods used in the fusion process steps may have an impact on fiber performance. Stripping of polyimide can be done by acid, knife, plasma discharge, or laser. Cleavers can hold the buffer or the cladding and optionally back-stop support the cleaving site. Splicers can use plasma or thermal heaters with variable application and timing of heating conditions. Re-coaters can use UV cured acrylics or thermal cured polyimide. We have explored a variety of fusion splicing process methods using a range of commercial products and tested their impact on performance. The exploration included working at vendor facilities with a field FRD testing apparatus to provide feedback for process optimization. Figure 7 shows results from the fiber splice tests using the 120um core FBP fiber. Our results show that the fusion splicing process can be tuned to yield a 0.15° to 0.20° increase to collimated FRD, achieving a final FRD value of ~1.5°. While the fiber can be recoated with no impact on FRD, shrink wrap style splice cover sleeves do degrade the performance. We measured a bulk throughput loss due to a single splice of ~0.6 % and loss from two splices in series of < 1%, working at 850 nm and using the full numerical aperture of the fiber. Loss measurements were made relative to a fibre before it was cut and re-joined with splicing. Our conclusion is that fusion splicing is a viable scheme for high throughput, low FRD fiber connections.

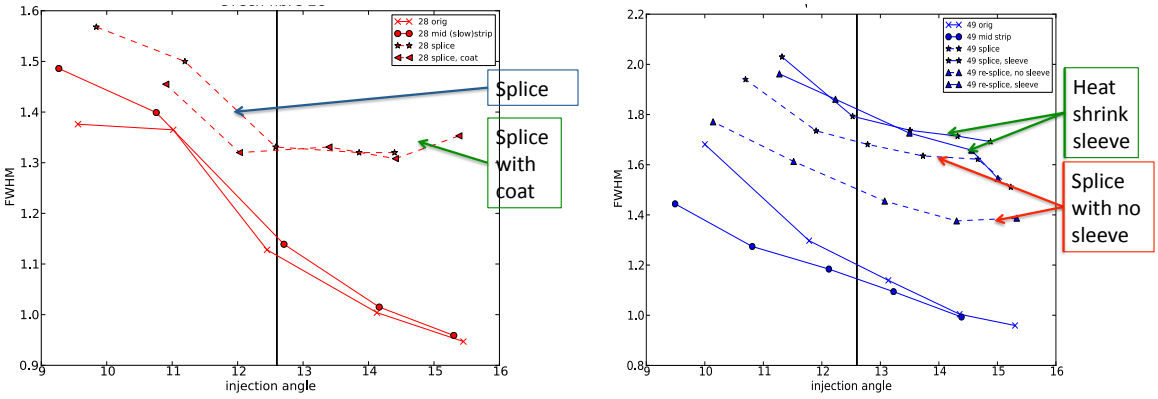

Figure 7 The effects of stripping, splicing, re-coating, and heat-shrink sleeving on fiber FRD. The curves show the collimated FRD ring width (degrees FWHM) as a function of injection angle. The thin vertical line corresponds to the BigBOSS maximum injection angle at f/4.5. Pre-splice measures are shown with a solid line + "X". Stripped fibers, pre-splice are shown solid line + circles. Spliced fibers are shown by dashed lines. FRD measurement error is ~ 0.1°. Stripping and coating have no significant effect on FRD. Splicing and shrink sleeving increases FRD by 0.2 ° to 0.4 °.

5 FIBER CABLE, JUNCTION BOXES & ROUTING

Actuator fibers from the focal plane's rear face are collected via junction boxes into ten fiber cables that are each routed ~ 40m to a spectrograph slit. Requirements for the cable and its routing include:

Sub-bundle maximum cross-dimension for focal plane routing 32 mm
Accommodate 15mm translation each axis between the focal plane and telescope structure
Accommodate telescope polar and declination rotations
Accommodate cable rotation required for installation
Accommodate fiber splicing connection
Robust to repeated flexing (30k cycles)
Operational temperature range -10^{o} to +20^{o}C

As illustrated in Figure 8, the fibers from localized actuators regions will be collected into sub-bundles supported by a harnessing grid located near the focal plane's back surface and then routed across the corrector support spider to fiber junction boxes which are attached to the primary focus support ring. The routing includes strain relief loops to accommodate the 15mm differential motion between the focal plane and the support ring. The fiber cable, illustrated in Figure 9, uses an Aramid yarn tensile element to limit length extension and is built up with a polymer coating to a diameter around which the loose-fiber carrying furcation tubes can be spiral wound in a uniform radial packing. The spiral wrap avoids cumulative tension at the fiber terminations due to differential length strain when bending the conduit. The helical cable core is wrapped with a protective ribbon of polymer tape and a hygroscopic gel layer to maintain a dry environment within the cable volume. We intend to use ten primary cables consisting of industry standard 25 mm conduits, each supporting 32 furcation tubes, 3 mm in diameter, that carry loose-packed (<80%) fibers. Cable management assemblies are used to ensures that the cable motions are well-defined and in pure bending at a defined radius. The cable management scheme and two telescope axis pivots are described elsewhere in these proceedings[5]. The cable junction boxes are used to collect individual actuator fibers into a fiber cable and include free loops of fiber that equalize differential fiber tension within the main cable, relieve fiber to cable differential thermal expansion, and isolate longitudinal fiber movement. Cable junction boxes will also be located in the spectrograph room to provide a similar reservoir of fiber length to the instrument slit assemblies. The junction box fiber loops can be pulled from the boxes to reach fiber splicing equipment and also include provision for strain relief mounting of fiber splices.

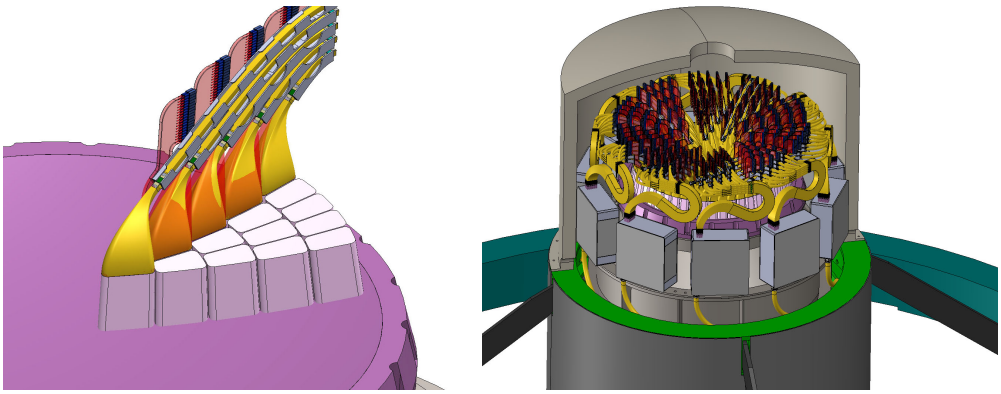

Figure 8. Fibers and wires are collected from the back of the focal plane (left image) in sections containing 32 actuators. The fibers are collected into cables at 10 junction boxes arranged about the focal plane (right image).

6 FIBER SLIT ARRAY

The output end of the fibers terminate into 10 slit arrays, one per spectrograph assembly. Each slit array consists of a group of 500 fibers arranged in a 500 mm radius planar arc specified by the spectrograph optical prescription. Optical tolerances demand a precise location for the fiber tips with respect to focal distance, i.e., the fiber tips must lie within 50 μm of the desired input focal surface. Lateral and fiber center spacings locations are far less demanding. The fiber axis diverge from a radial center in order to form a common spectrograph entrance pupil.

The primary fiber slit requirements include the following:

500 fibers per slit
Fiber spacing 260 μm
Slit radius of curvature 500 mm convex
Fiber ends located to ±50 μm of radius of curvature
Fibers' optical axis diverge from common 500 mm radius to illuminate pupil.
Fiber ends AR coated (360–980 nm) <1.5% loss
Operational temperature range 15° to 25° C

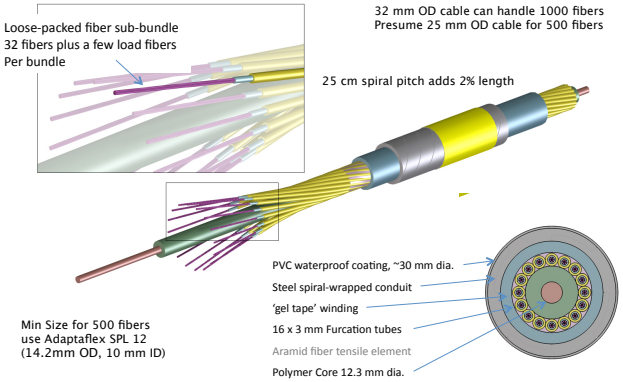

Figure 9. The fiber cable is constructed of multiple layers including tnsile and buffer elements as well as spiral wrapped sub-bundles of furcation tube containing the optical fiber.

Each slit array will be fabricated from four 125-fibers modules that have been precisely arranged on an assembly plate. The plate provides the mechanical interface to the spectrograph and is installed using registration pins for accurate location. The assembly plate also supports and constrains each block's fiber bundle and terminates the bundles' protective sheaths. The ends of the individual fibers are bonded into V-grooves machined at radial angles that point each fiber toward the radius of curvature. The fiber ends are cleaved and then co-polished with the block surface. An anti-reflection coated thin plate of fused silica is bonded over the curved slit surface using optical index matching cement. The jacketed fiber is supported by low modulus adhesive on a free bonding ledge to enforce minimum curvature radii and to strain relief the fibers before their entry into bundle sleeving.

7 CONCLUSION

The BigBOSS fiber optics systems accommodate the 5,000 object multi-object spectrographs needed for cosmology observations to explore dark energy. The fiber system design and performance requirements have been established and a fiber measurement system used to characterize and explore fiber connection methods. Optimized fusion-splicing appears to deliver superior optical performance fiber connection than does mechanical methods.

ACKNOWLEDGMENTS

This work was supported by the Director, Office of Science, of the U.S. Department of Energy under Contract No. DE-AC03-76SF00098. Andrew Vanderburg assisted with fiber performance measurements.

REFERENCES

[1] Mostek, N., et al, "Mapping the Universe with BigBOSS", Proc. SPIE 8446-24 (2012).

[2] Sholl, M.J., et al, "BigBOSS: A stage IV dark energy redshift survey," Proc. SPIE 8446-237 (2012).

[3] Jelinksy, P., et al, "The BigBOSS Spectrograph", Proc. SPIE 8446-238 (2012).

[4] Boucher, D., et al, “Step-Index All-Silica Fibres with Enhanced Transmission in a Broad Spectral Range”, IOAI, 109 (1997).

[5] Besuner,R., et al, “Integrating BigBOSS with the Mayall Telescope”, Proc. SPIE 8446-194 (2012).